

Development of a computational biomechanical  
model of the human upper-airway soft-tissues  
towards simulating obstructive sleep apnea

Pelteret, J-P. V.\*<sup>†</sup> and Reddy, B. D.\*

\*Centre for Research in Computational and Applied Mechanics

Mechanical Engineering Department

University of Cape Town

<sup>†</sup> email: [jppelteret.uct@gmail.com](mailto:jppelteret.uct@gmail.com)

University of Cape Town,

5th floor, Menzies Building,

Private Bag X3,

7701 Rondebosch,

Cape Town,

Western Cape,

South Africa

phone: + 27 21 650-3817

# Development of a computational biomechanical model of the human upper-airway soft-tissues towards simulating obstructive sleep apnea

## **Keywords**

obstructive sleep apnea; tongue; human upper-airway; computational model;  
skeletal muscle model; neural model; finite-element method

## **Summary**

In this paper, we present details of the construction and development of a soft-tissue model of the human upper-airway, with the ultimate goal of simulating obstructive sleep apnea. The steps taken to produce a representative anatomical geometry, of which the associated muscle histology is also captured, is documented. An overview of the mathematical models used to describe tissue behaviour, both at a macro- and micro-scopic level, is given. A neurological model, which mimics the proprioceptive capabilities of the body, is described as it is applied to control the active dynamics of the tongue. A simplified scenario, which allows for the manipulation of several environmental influences, is presented. Insights into the characteristics and functioning of the tongue, and in particular the genioglossus, during inhalation are given. Furthermore, it is demonstrated that the model has merits in understanding the active response of the tongue to changing physical conditions.

# 1 Introduction

Obstructive sleep apnea (OSA) [Malhotra and White, 2002, Ryan and Bradley, 2005, White, 2006, Davidson, 2008, Waite, 1998] is a syndrome of increasing prevalence in modern society. Characterized by a partial or complete reduction in airway patency, the collapse of the upper airway leads to brief or, in the case of severe OSA, extended periods of hypoxia. During the process of restoring airway patency, the patient often performs violent movements. Collectively, these lead to a reduction in the quality of sleep. Although it severely reduces the quality of life of the patient [Dalmasso and Prota, 1996, Hamans et al., 2000], OSA is not necessarily life-threatening in itself. However, associated with this disorder are many secondary effects [Waite, 1998], such as those of a cardiovascular nature [Buchner et al., 2007, Butt et al., 2010], which may have more severe direct consequences. Many treatments, such as CPAP [Buchner et al., 2007], oral appliances [Millman et al., 1998, Clark, 1998, Ono et al., 1996, Ryan et al., 1999], electrical stimulation [Hu et al., 2008] and surgical intervention [Madani, 2002, Johnson and Chinn, 1994, Waite, 1998] have been evaluated and used to correct the syndrome.

Numerous difficult challenges face researchers trying to understand the complex pathophysiology [Fogel et al., 2004, Isono et al., 2003, Remmers et al., 1978, Rubinstein et al., 1988, Waite, 1998] of this disorder. The upper airway is an intricate structure of tissues, with functions, behaviours and interactions that are complex to describe and predict. Physical factors, ranging from posture [Battagel et al., 2002, Ingman et al., 2004, Ozbek et al., 1998, Tagaito et al., 2010] to pharyngeal length [Segal et al., 2008, Pae et al., 1997] and geometry [Ayappa and Rapoport, 2003, Froberg et al., 1995, Isono et al., 1997] have been linked to OSA. The breadth of anthropomorphic and physiological variation between individuals is wide and, although risk factors for OSA (such as gender [Malhotra

et al., 2002a], obesity [Carrera et al., 2004, Waite, 1998] and body-mass index [Mayer et al., 1996], age [Veldi et al., 2001] and nasal obstruction [Rappai et al., 2003, McNicholas, 2008]) are well known, there exists no clear mechanism other than individual sleep studies for detecting this disorder.

Much experimental work has been performed exploring the pathophysiology of OSA. The role of the muscles of the tongue have been well described, with much of the focus of experimental research in this area centered on the genioglossus, which acts as the airway dilator for the tongue. Its role in response due to changing airway pressures in healthy adults and OSA suffers has been heavily documented [Akahoshi et al., 2001, Malhotra et al., 2000, 2002b, Stanchina et al., 2002, Pierce et al., 2007, Oliven et al., 2007, Isono et al., 1999]. However, a definitive characterisation of the influence of other muscles has not been performed due to the complexity of the anatomy of the tongue.

To this end, computational models can provide valuable insight into the functioning of the tongue and the influence of the airway dynamics on its motion. These models are mathematical representations of the anatomy, with geometrical descriptions of the tissues being coupled to models that predict the response of the tissues to forces that act upon them. Provided that a representative model can be constructed and the surrounding environmental conditions described with sufficient accuracy, these models may enhance understanding of the influence of various conditions which may not necessarily be able to be investigated experimentally. In order to produce such a model, an accurate description of the geometry of the human upper airway must be constructed. Furthermore, the underlying histology of the various tissues should be considered and their influence accounted for within the model. The models that govern the response of the tissues are often directly correlated to experimental analysis performed at the macro- and microscopic levels.

Ultimately, the goal might be to produce such a model that can be fitted to any specific individual, thus facilitating predictions and analysis on a patient-specific basis and thereby finding use in clinical applications. However, this goal is challenging due to the idiosyncrasies in an individual’s anatomy and physiology, and few such examples pertaining to the human upper-airway soft-tissues exist [Lloyd et al., 2012]. Computational models of the tongue and its surrounding tissues have thus far found application in the study of respiratory mechanics [Huang et al., 2005a,b, 2007], muscle kinematics [Gérard et al., 2003, Vogt et al., 2006, Wu et al., 2006, Buchaillard and Perrier, 2009, Stavness et al., 2011], speech production [Wilhelms-Tricarico, 1995, Sanguineti et al., 1998, Fang et al., 2009] and the prediction of the effects of surgical interventions [Fujita et al., 2007, Huang et al., 2007]. It is important to note that, for the most part, each of these models has a very specialized construction and have been implemented in entirely different ways.

The work presented here provides a synopsis of the methodology utilized to construct a model of the tongue and surrounding tissues. We describe a method in which mathematical descriptions of muscle functioning and neural response can be used in conjunction with a geometric model. This model, the mathematical details of which can be found in [Pelteret and Reddy, 2012] and a simplified version in [Kajee et al., 2013], is shown to produce a physiologically realistic prediction of muscle activation resulting in position control of the tongue under complex loading conditions. We demonstrate how this model can be used to understand the effect of physiological and environmental influences on the behaviour and response of the tongue musculature. An analysis of the effect of posture, pressure loading and certain physiological parameters on the response of the genioglossus is presented.

## 2 Model construction

### 2.1 Imaging

The Visible Human Project (VHP) [U.S. National Library of Medicine, 2009, Spitzer et al., 1996] is an open repository consisting of complete adult human radiological and photographic data sets obtained over several years. To this date, three specimens have been cryogenically preserved and have subsequently undergone full magnetic-resonance imaging (MRI) and X-ray computed tomography (CT) scans. Following these imaging procedures, the specimens have been transversely sectioned (and destroyed in this process), and colour photographs of each section made. As with the MRI and CT imaging processes, it had been methodically ensured that both the sectioning and photographic processes occurred in a single, parallel axis. Having the three consistent imaging sources provides researchers with a unique view to be able to identify anatomical structures within the body by utilising the strengths of each technique to offset the weaknesses of the other.

The head and thorax of the female photographic data set, which is utilized in this work, consists of 1203 sections each of 2-megapixel resolution. This translates to a per-pixel resolution of  $\frac{1}{3} \times \frac{1}{3}$  mm, with the distance between each section equal to  $\frac{1}{3}$  mm. The corresponding MRI and CT data is of significantly lower resolution and was therefore not considered, as the requirement for capturing fine detail in the anatomical structures was deemed vital. Selected slices in the head and upper torso were used in conjunction with the commercial software package MIMICS [NV, 2010] to navigate the two-dimensional photographs in three dimensions. The 2-d images, which were aligned in the capturing procedure, are effectively “stacked-up” on one another and build up a volumetric data set which can be re-sectioned in any of the medical view planes. Figure 1 depicts

a cropped view of an original photograph, along with one that is a selected group of voxels (3-d pixels) extracted from multiple transverse sections in order to produce the coronal section as a specified position in space. Critically, the photographic detail is sufficient to provide insights into the muscle fibre histology that constitutes the tongue. In both figures 1a and 1b, the directionality of the underlying muscle fibres can be seen. Although modern techniques such as diffusion tensor imaging (DTI) [Gaige et al., 2007, Shinagawa et al., 2008] can be used to visualize these structures, traditional MRI and CT imaging, both of which remain vital in understanding OSA [Schwab et al., 2003, Caballero et al., 1998, Vos et al., 2007, Brennick et al., 2004, dos Reis Zinsly et al., 2010], cannot capture these features.

## 2.2 Data extraction

The ultimate goal of the reconstruction process is to reproduce a representative volume that approximates the geometry of the desired anatomy. This entails defining regions on each cut-plane that are part a specific anatomical feature, a task known as *masking*. The collection of the 2-d selections over numerous planes then constitutes the extracted part. The traditional approach to producing models from data sources of this nature would be to exploit the nature of the imaging process to automate this process. Algorithms, which distinguish features through colour comparison, have been developed to perform these tasks. However, due to the nature of the human anatomy, these methods cannot be used in conjunction with photographs. As is observed in figure 1, adipose tissue, bone, cartilage and ligaments appear similar in the grey-scale colour spectrum. The presence of background information, that is, anatomy visible through the open airway which does not exist on the selected view-plane, further complicates the reconstruction process. Thus, with reference to the anatomical literature

[Davies, 1967, Mortley, 1972, Agur and Dalley, 2005], this task was performed manually for the numerous soft-tissues of the human upper airway. Figure 2a demonstrates the definition of various tissues of and surrounding the tongue on the sagittal plane. Due to the nature of the computational implementation used to simulating the soft tissues, it was not necessary to discriminate between the adjacent muscular tissues. For this reason, the bulk tissue that constitutes the tongue floor, and the intrinsic and extrinsic muscles of the tongue, was defined by a single volume. Simultaneously, information regarding the fibre directions for muscular substructures was defined using the same commercial package. For each muscle, regions approximated as having the same gross direction were specified by a geometric primitive, namely a cylinder. The spatial position of the end-points of each cylinder were chosen by approximating the trajectory of each fibre-bundle through all three view-planes. A multitude of cylinders, an example of which is illustrated in figure 2b, were used to define collectively each muscle of the tongue.

Due to the complexity of the tongue histology and the relative coarseness of the photographic data-set, some of the muscles did not prominently feature and could not be observed to a high degree of confidence. Guided by the literature [Davies, 1967, Mortley, 1972, Agur and Dalley, 2005, Abd-El-Malek, 1939, Takemoto, 2001], the position and directionality of these muscles was inferred relative to the more visible musculature.

The process of developing both the volumetric and fibre data sets for soft tissues was an iterative one. The presence of the background artifacts at the edges of each tissue region required numerous checks between all three views and subsequent corrections in order to arrive at an acceptable description of the anatomy. To minimize the duration of time taken to produce the result, a skeletonization technique was used to rapidly sketch out the approximate shape

of the part for evaluation. To achieve this for any chosen part, only a few sections on each plane were filled, while the others were temporarily neglected. This process is illustrated in figure 3a. The intermediate representation for the epiglottis, as produced using this method, is depicted in figure 3b. Once a satisfactory outline of the feature is developed, the skeleton frame acts as a set of markers for the borders of the external surface of the part from while the rest of the view-planes can be filled to produce the final model.

A section of the completed volume that is used to represent the tongue is presented in figure 3c. It can be observed that this volume encapsulates not only the constituent micro-histology of the intrinsic and extrinsic tongue musculature, but also the surrounding muscular and glandular tissues.

A similar process of initial simplification and subsequent refinement was used to develop the structure of the muscle fibres. Initially, the volume occupied by each component muscle of the tongue was defined. Although this data is later discarded, it served as an initial platform of reference to determine whether the underlying histology of the tongue, as interpreted from the photographic data, was accurate. Using the defined muscle volume regions, the task of interpreting the interweaving sub-structures in conjunction with the literature was made significantly easier. Prominent muscles such as the genioglossus required little effort to define; figure 4a depicts the uniformity of the structures used to capture its histology. For spatially intricate muscles such as the verticalis shown in figure 4b, a broad outline of the muscle was first developed using volumetrically sizable cylinders. Once these demonstrated that the gross description of the muscle was acceptable and that the distinguishing features had been captured, they were reduced in size and the local directionality, which may change rapidly from point to point, corrected.

The mathematical entities used to describe directional quantities such as

those of the fibres require a consistent definition for the cylinder start and end points in order to produce the correct direction field for the completed model. This is somewhat contrary to the way that muscles work, in that their fibres are orientation-agnostic and contract in an “axial” direction, which could equally be defined parallel or anti-parallel to the center-line of each fibre bundle. As this was not possible during the construction phase, the final step in the production of the fibre data-set was to ensure that they were consistently defined in this manner.

In figure 5 we provide insight into the detail of the raw geometry of the upper-airway tissues that was extracted from the imaging data. It can be observed that the resting position of the subject was such that the tongue positioned far forward in the mouth and was clamped down by the teeth. Furthermore, the tongue was in close proximity to- and, in some regions, in contact with- the hard- and soft-palate. These features, clearly not aligned with the natural posture of the oral anatomy at rest or during sleep, illustrate shortcomings of the model that have to be considered when interpreting any simulation results.

## 2.3 Reconstruction procedure

To complete the construction of the anatomical model, the 3-d model was transferred to specialist CAD software, ICEMCFD [Inc., 2010], equipped to describe the model in such a way that it could be used in conjunction with software specifically developed to model the soft- and hard- biological tissues and represent muscle behaviour. As the human anatomy is not truly symmetric around the mid-sagittal plane, as was observed in this data-set, a full representation of the extracted anatomy was constructed, with the asymmetries included.

Furthermore, there exist some difficulties in the direct inclusion of some

anatomical features. For example, consider the styloglossus, which has its origin at the styloid process and stylohyoid ligament and inserts in the side and inferior aspect of the tongue. This muscle, contained within a collagenous sheath, follows a path through to numerous other muscle groups and various other tissues. As these tissues are not of the same constitution, a geometrically complex representation of these interfaces must be produced. It also interacts with these tissues in a manner that is complex to represent mathematically; due to their contact, both it and the adjacent tissues exert a mutual pressure on one-another. This allows the tissues to support one another, but also induce hydrostatic changes within one another as muscles deform, contract and relax. The sliding motion of the muscle within its sheath is also not void of friction. Should these features need to be captured, the extent and complexity of the geometric and numerical model, and therefore the time required to simulate it, would increase considerably.

The alternative to representing such a feature is to remove it completely and replace it with a simplified analogue that captures the essence of the feature. Figure 6 demonstrates the result of removing the styloglossus from the model. The muscle, for which we would need to further describe a support structure of adjacent tissues, is completely neglected from a volumetric perspective. However, as will be described in sections 2.4 and 3, the effect of contraction of this removed region of muscle was approximated. Similarly, feature removal dictated that the digastric and stylohyoid muscles be represented in an alternative manner. These two muscles, which insert into the tongue floor and hyoid bone respectively, again have geometrically complex paths and interactions with multiple structures which themselves, independent of their connectivity to the rest of the anatomy, are difficult to incorporate into the model.

## 2.4 Features of the completed model

Subsequent to the final CAD reconstruction, the volume of each material is subdivided into numerous sub-volumes, known as “cells”, which are later used in the process of computational modelling of the anatomical system. The geometric complexity of the model greatly influences this process and ultimately the quality of the results produced by the model. Figure 7 illustrates the completed anatomical model that was used in this work. Five major anatomical components are represented here: The muscular tissue of the tongue body (incorporating both extrinsic and intrinsic muscles as well as the sublingual glands) and the tongue floor, the lower region of the mandible which serves as a fixture point for the lower tongue, the floating hyoid bone, a collection of adipose tissue and the glottal bursar both posterior to the hyoid bone, and lastly the cartilage of the epiglottis which rests on this adipose tissue.

Coupled with the gross anatomical model is one describing the underlying histology of the muscular tissues. This information is described as an additional layer of data within the model. The granularity of the macroscopic model determines how well this data is translated into the model, as the histological data is represented at the numerous spatially-defined calculation points within each cell. The representation of the various muscles groups that compose the tongue, viewed in the detail that the model captured, is shown in figure 8. Overall, 13 neurologically-distinct muscle groups are represented, with 5 of them having two components divided laterally on the mid-sagittal plane. Aligned with descriptions given by [Miyawaki et al., 1975] and the works of [Buchaillard and Perrier, 2009, Dang and Honda, 2001, Gérard et al., 2003], it is assumed that the genioglossus consists of three functional units. Due to the neurological (as opposed to physiological nature of the division of this muscle, it is not discussed in [Davies, 1967] or other physiology literature.

In general, during the process of the CAD model construction, various small geometric features are smoothed over as the description of the surface and interface curvature between parts cannot be captured in full. A single, purposeful modification was made to the tongue blade in order to reverse the deformation present due to its contact with the teeth. It was therefore thickened near its tip and at the same time the curvature of the region was modified to ensure a high quality of the numerical representation of this region.

### 3 Mathematical description of anatomy and physiology

A specialized mathematical methodology must be employed to solve the equations that later constitute the mathematical model. Of the numerous techniques available for use, the Finite-Element method (FEM) [Hughes, 2000] is most appropriate in this application. The basic principle behind these methods is that, given any set of conditions, the unknown solution of the system which we wish to determine coincides with its lowest-energy configuration. Coupling fundamental physical precepts, namely the conservation of linear momentum, conservation of mass and the second law of thermodynamics (in the form of constitutive models), with FEM we are able to ascertain an approximation to the correct state of the physical body being modelled under almost any conditions. In essence, this process involves the subdivision of the physical domain into cells and the determination of the solution to a function prescribed on each subdomain. This decomposition is illustrated in figure 7, where the domain is divided into numerous connected hexahedral cells.

In order to complete the description of the human upper-airway, it is necessary to couple the geometrical representation of the tissues with a mathematical model, known as a constitutive model, that describes how the tissues behave. The material parameters in such representative models are generally obtained from experiments.

Within this geometry are numerous materials that exhibit very different behaviours. For example, bone is very stiff in comparison to passive muscle and does not demonstrate any measurable directional preference (i.e. it behaves isotropically). However, histologically, bones remain a complex structure composed of the dense cortical outer layer with a porous interior made of trabecular bone.

Furthermore, unlike bone, muscular tissue is nearly incompressible, meaning that it undergoes no volume change during deformation. Therefore, a pragmatic view should be taken to determine which features of the histology are worth retaining in the context of the scenario being modelled, and which can be discarded in the interest of simplicity without compromising the accuracy of any results. To this end, most care was taken to best represent the most compliant materials, while simple constitutive models were used for the stiffer materials.

From a macroscopic viewpoint, that is at length scales of the reconstructed geometry, bone is isotropic and was not expected to experience significant deformation. The cartilage core of the epiglottis is similarly far stiffer than adipose and muscular tissues. Thus, both of these tissues were represented by simple single-parameter constitutive models with parameters selected from literature [Peterson and Bronzino, 2008, Reilly and Burstein, 1974, Li et al., 1999]. Adipose tissue, significantly more compliant than bone or cartilage but also isotropic, exhibits the behaviour that it becomes exponentially stiffer as it is stretched or compressed. Thus a different mathematical representation, again fitted to experimental data [Erdemir et al., 2006, Farvid et al., 2005], was utilized for it.

### 3.1 Muscle tissue

In order to motivate the functional models of active muscular tissue, it is required that one examine the composition and behaviour of the tissue from a number of perspectives. The muscles of the tongue are composed of skeletal muscle tissue. Visible in figure 1 as striations in the tongue are collections of muscle fibre bundles, or fascicles, which have diameters of the order of  $20 - 80\mu m$  [Stal et al., 2003]. A number of fascicles are encapsulated in a sheath of connective tissue, the epimysium, while each fascicle itself is further

surrounded by connective tissue known as the perimysium [Fung, 1993, Fox, 2006]. Separating muscle fibres is connective tissue as well as adipose tissue of varying concentrations [Miller et al., 2002]. Each muscle fibre is composed of numerous myofibrils, which have diameters of the order of  $1\mu m$  and extend the length of the fibre. The interstitial space between the myofibrils is filled by sarcoplasm. In the microscopic section of stained tissue presented in figure 9, fascicles of two interweaving muscle groups of the tongue and the surrounding interstitial tissue can be seen. Myofibrils can be further subdivided into myofilaments which are each approximately  $2.5\mu m$  long, dependent on the state of excitation of the muscle. Sarcomeres, the smallest functional unit of muscular tissue, are of the order of  $2.2\mu m$  in length and are arranged serially and in parallel to constitute the myofilaments.

In figure 9b, a parallel collection of sarcomeres attached to two dark bands, known as Z-discs, are visible. Of the three proteins that constitute the rest of the sarcomere, two, namely titin and actin, are directly attached to the Z-disc. The thin titin filament, which has elastic properties, holds the myosin filament in place. From the myosin protrude cross-bridges which, as described by the *cross-bridge theory* are by the process of chemical activation the direct cause of muscle shortening. Situated between adjacent titin filaments is the actin filament, on the surface of which exist binding sites for the cross-bridges. The actin-myosin complex, which is collectively responsible for the active contraction of the sarcomere, exists within the two grey A-bands visible in the image while the white I-bands into which this complex can move consists of titin and actin alone.

Three further physiological properties of muscles that affect its functioning also require consideration. Skeletal muscle can be classified into two main types, namely fast- and slow-twitch. Both of these fibre-types are present in the tongue

and are recruited separately to produce different motions. Pennation, where the line of action is not parallel to the axis of the muscle fibres, does not exist within the tongue musculature.

Fundamental experimental analysis has resulted in the understanding of the force-generation characteristics of active muscle at both macro- and microscopic length scales. The seminal work conducted by [Hill \[1938\]](#) produced the force-velocity relationship for tetanized skeletal muscle in an isotonic condition. It was demonstrated that an inverse relationship exists between the generated contractile force and the velocity of contraction, and that muscle preload affects this relationship. Huxley later proposed the sliding filament theory [[Huxley, 1974](#), [Fung, 1993](#)] which described the functioning of the actin-myosin complex. Isometric studies have been used to describe the length-tension relationship [[Gordon et al., 1966a,b](#)]. Results have demonstrated that the initial stiffness exhibited by activated muscle is due to the elastic elements of the sarcomeres, while at high magnitudes of elongation the stiffness is related to the rate of binding and breakage of cross-bridges [[Cole et al., 1996](#)]. At high stretches, the stiffness of the connective tissues, such as the epimysium, dominate while the muscle can no longer produce contractile force. This effect of the latter can be quantified by studies on passive tissues, such as those documented in [[ter Keurs et al., 1978](#)]. From this information, the force-length relationships within individual sarcomeres, relating the effectiveness of the sarcomere to produce contractile, have been deduced and related to the physical conditions present within it. They function optimally at near resting length when the cross-bridges are in the vicinity of the maximal number of binding sites [[Fox, 2006](#), [Herzog and Ait-Haddou, 2002](#)]. At high degrees of compression, the I-band disappears and leaves no space for further contraction, while at large stretches all of the cross-bridges become detached. In both cases, the muscle no longer produces shortening force.

### 3.1.1 Representative functional model for active skeletal muscle

To successfully model the active dynamics of muscular tissue, we choose to utilize a representative model which emulates the response of a localized region of tissue without directly resolving all of the complexities of the physiology. Three models of this nature are commonly utilized in muscular modelling. *Cross-bridge theory* [Fung, 1993, Peskin, 1975, Zahalak and Ma, 1990, Williams, 2011], a mathematical representation of the sliding-filament theory, is a statistical model which associates the generated contractile force with the number of attached cross-bridges. It has been demonstrated to provide an excellent representation of the mechanics of individual sarcomeres; see [Mijailovich et al., 1996, Cooke et al., 1994, Rassier et al., 2003, Wu and Herzog, 1999] for examples of its use. An extension of this model is the *distribution moment model* [Zahalak and Ma, 1990, Fung, 1993] that accounts for effects of calcium activation on the cross-bridges. Both of these models are highly complex and describe the functioning of the sarcomere on the chemical level.

In contrast, the phenomenologically-derived *Hill model* is the most widely adopted model to represent the mechanics of bulk muscle-tissue and musculo-skeletal systems. Taking numerous formats, the three-element Hill model shown in figure 10 is used to approximate the dynamics of a collection of sarcomeres. This model, which leverages the organisation of the sarcomeres and the surrounding tissue, ultimately describes the tissue at the fibre level. The three elements are arranged so that the active contractile unit (CE) is in-line with the series element (SE), both of which are lateral to the parallel element (PE). The PE and SE may be chosen to represent the passive physiology of the surrounding muscular tissues (respectively the stiff epimysium and perimysium, and the intrinsic elasticity of the Z-discs and titin filaments). Due to a fundamental assumption that all of the sarcomeres in a selected region of tissue behave identically, the

CE thus represents the collective response of the active sarcomeres through the entire region. In particular, the CE represents the active actin-myosin complex at a high level, with its mathematical description incorporating the force-length and force-velocity relationships as well as a component interpreted as the neurological input to the muscle.

The skeletal muscle model presented by [Martins et al. \[1998, 2006\]](#) has been adapted and extended to provide a mathematical representation of each of these elements. Muscle models of this nature have been used to represent the functioning of the tongue [[Wilhelms-Tricarico, 1995](#)] as well as pelvic [[D'Aulignac et al., 2005](#)] and arterial [[Holtzapfel et al., 2000](#), [Humphrey and Yin, 1987](#), [Humphrey et al., 1990](#)] models from which this methodology is derived. Model parameters describing the matrix [[Sanguineti et al., 1998](#), [Van Ee et al., 2000](#), [Gérard et al., 2003](#), [Perrier et al., 2003](#), [Dang and Honda, 2004](#), [Huang et al., 2005a](#), [Van Loocke et al., 2006](#), [Vogt et al., 2006](#), [Buchaillard and Perrier, 2009](#)] and fibre composition, in terms of the volume fraction [[Lieber et al., 2003](#), [Humbert et al., 2008](#), [Miller et al., 2002](#)], passive [[Hill, 1953](#), [Martins et al., 2006](#)] and active [[Hill, 1938](#), [Fung, 1993](#), [Johansson et al., 2000](#), [Herzog and Ait-Haddou, 2002](#), [Lieber, 2002](#)] elements, were chosen to be representative of experimentally attained data.

### 3.1.2 Neural model

Muscle contraction occurs through a complex electro-chemical and mechanical event facilitated by the delivery of specific chemical substances at nerve endings. The activation of a varying number of neurons through impulses delivered to each myofibre by a somatic motor nerve causes the recruitment of a varying number of muscle fibres and therefore a gradual and controlled contraction event. In an event known as a twitch, the muscle fibres contract for duration of impulse, and relax thereafter. A collection of successive twitches, each of

which results in a minor reduction in length of the I-band, leads to the overall shortening of the muscle. The strength of the contraction depends on the frequency and overall duration of the impulses.

In this work, we utilized the neural model presented by [Pandy et al. \[1990\]](#), [Pandy \[2001\]](#) to model muscle excitation. This model captures the delay between muscle excitation and activation, approximating the chemical changes in the tissue. The benefit to utilising such a model is that its input consists simply of a single value which determines whether the muscle contracts or relaxes. To simplify the description of the control mechanism over all fibres which constitute a single muscle group, we assume that they all receive an identical signal simultaneously. However, this does not imply that the force-generation properties are homogeneous throughout the muscle; this remains collectively defined by the local deformation conditions and the Hill-model.

Although the inputs to the excitation model can be prescribed, we wish to simulate conditions that change as the tongue and the surrounding tissues move. Due to the complex models which govern its motion, describing these inputs *a priori* is a challenging task [[Sokoloff, 2004](#)]. EMG studies, such as those performed by [Akahoshi et al. \[2001\]](#), [Malhotra et al. \[2000\]](#), [Stanchina et al. \[2002\]](#), [Pierce et al. \[2007\]](#), provide valuable insights into the functioning of the tongue. These works demonstrate the response of the genioglossus to the changing airway pressure that develops during breathing. For example, the tongue model developed by [[Huang et al., 2005a](#)] used a non-linear relationship between the genioglossus activation level and epiglottal pressure, deduced from experimental results, to represent the genioglossal response to simulated breathing during wakeful and sleeping conditions. However, due to the representation of the entire tongue histology, the collective EMG data is not enough to drive a model the nature of that used in this work, as no information regarding

the neurological response of (many of) the other muscle groups is available. Furthermore, the conditions under which the experimental studies were performed differ, and describing consistent and accurate conditions is difficult.

To this end, we have developed and incorporated a neurological model which responds to an *a priori* unknown load and determines an appropriate neurological and muscular response to the applied load. In this way, the tongue gains a degree of proprioception or spatial awareness and is able to determine which muscles to activate in order to achieve a prescribed configuration. In particular, we dictate that the tongue must resist movement under load and retain its initial configuration. This is achieved by measuring the displacement of a number of points on the surface of the tongue and using a mathematical construct known as a genetic algorithm [Goldberg, 1989, Haupt and Haupt, 2004, Mitchell, 1999] to minimize the overall displacement of these points. This technique, which mimics the evolutionary processes of biology, selects and tests the result of the activation of a selection of muscle groups at a single snap-shot in time, at which the loads are defined and constant. It then determines which of these combinations produce the best results and recombines their traits to form a new selection of active signals to be tested. After this process is repeated several times, the best choice for the active set of muscle signals is made and this is applied to control the muscles at that instant in time. The effectiveness of this approach is demonstrated in section 4.

## 3.2 FEM implementation and simulation methodology

### 3.2.1 Implementation

This work has been implemented using the open-source `deal.II` [Bangerth et al., 2007] framework in conjunction with additional high-performance software libraries [Wall, 2010, Heroux et al., 2005, Int, 2011, Karypis and Kumar, 2009].

In particular, we utilize the methodology described in [Simo et al., 1985, Simo and Taylor, 1991, Miehe, 1994] to determine the correct configuration of the system under load, while successfully ensuring that the incompressibility of the biological materials is retained. We account for the finite-volume occupied by each muscle group using an approximation of the method presented by Baaijens et al. [2010], Driessen et al. [2005], van Oijen [2003]. In doing so, we assume that the proportion of the volume at any point occupied by muscle matrix (constituted by a collection of interstitial and adipose tissues) is uniform throughout the tongue; however, studies have demonstrate that this simplification is not strictly correct [Nashi et al., 2007]. We provide special treatment for the “external” muscles that were removed from the geometric model. Shown as a dense collection of lines in figure 8d, we assume that they can be represented by single Hill-element which results in loads that act on the boundary of the tongue. Their line of action extends from a single point of origin for each muscle to a calculation point on the tongue surface. Furthermore, we also make a very simple approximation for the pre-stressed condition of the tissues.

### 3.2.2 Condition of simulations

Anatomical constraints on the simplified geometry result from the truncation of the mandible and the interface between the thyroid cartilage and the adipose tissue superior to it. For the purposes of simplification, we assume that both of these surfaces undergo no motion at all, thus serving as fixture points for the rest of the anatomy.

Two environmental constraints that require consideration are the posture and the air-pressure loading derived from the state of breathing. Although we consider both to be variable, we define them in the following manner: By assigning a density to each material, we modify the direction of gravitational influence from that simulating an upright state (caudal orientation) to the supine

posture (dorsal orientation). To simulate breathing, we assume that the nominal value of the pressure load changes semi-sinusoidally between no-load and a epiglottal pressure of  $-500Pa$ , considered to be on upper limit of the pharyngeal pressure loss during inspiration [Van Hirtum et al., 2004] and marginally higher than the threshold for the stagnation of tonic and phasic activity of the genioglossus during sleep [Huang et al., 2005a]. In this manner, we simulate successive inhalations, with the process of exhalation being excluded. The spatial distribution determines the assumed source of the air-inlet. To simulate mouth breathing, we assume that the airway pressure decreases linearly from the tongue tip to its posterior surface, which is exposed to the epiglottal pressure. For nasal breathing, where the oral cavity remains closed, we assume that the pressure distribution is uniform over the entire surface of the tongue. In the case where the mouth is open but inhalation is made through the nose, the posterior surface of the tongue remains exposed to the low epiglottal pressure but the rest of its surface experiences atmospheric conditions, thus approximating the condition where the tongue and soft-palate make contact and seal off the oral cavity.

## 4 Results and discussion

We now present the results of a computational analysis of physical and environmental factors that affect the tongue and main airway dilator (genioglossus) response during inhalation. As a baseline example from which we can present the trends that will be investigated, we consider a case where the supine posture, oral inspiration and maximal epiglottal pressure of  $-500Pa$  is assumed.

In figure 11a, a comparison of the deflection of multiple points on the mid-sagittal plane on the geometry for a full-passive versus the actively controlled tongue are presented. It was observed that in the passive condition, the tongue experiences large displacements (approximately  $8mm$  and  $5mm$  at the tip and upper-posterior respectively) due to gravitational influences alone. The addition of airway-induced loads results in up-to a further  $3.5mm$  deflection, depending on the magnitude of the applied load. However, once the muscle control algorithm is utilized, the magnitude of this deflection is substantially damped. Due to limitations with respect to the degree of control that it can produce, tissue displacement remains; however, the  $1mm$  difference in displacement measured at position  $\mathbf{P}_C$  is within the bounds of  $2mm$  which was recorded by Cheng et al. [2008] during experimental analysis under similar conditions. Interestingly, maintenance of position control of the tongue results in control of the epiglottis position.

From the neurological model it is possible to quantify the strength of contraction that each muscle is predicted to require at each discrete point in time. However, this data exhibits oscillations in the response, due to the lack of fine-grained motor control in the neural control algorithms; such control is possible but the computational expense involved accounting for this is too large. We therefore filter these results, arriving at the smoothed response, which is close to that which the control algorithm attempts to achieve and around which raw data

oscillates. Figure 11b depicts the response of the muscle groups after a smoothing filter has been applied. In particular, plotted is a measure of the strength of muscle contraction in comparison to the maximum contractile response under possible isometric conditions, the fraction of full muscle response (FFMR). This is measured from a neurological perspective; local conditions for each set of sarcomeres determine how this is translated into the locally-generated contractile force.

A number of basic observations can be made about this data. It is clear that the response of all active muscles mimics that of the applied load: the response is semi-sinusoidal. The muscles which are required to produce the greatest forces to oppose the load are the medial and posterior part of the genioglossus, with the strength of contraction peaking between 1.5 – 2%; this is comparable to the EMG data available in the literature [Akahoshi et al., 2001, Malhotra et al., 2000, 2002b, Stanchina et al., 2002, Pierce et al., 2007], with the difference in predicted contractile strength explained by the choice of model parameters and conditions under which the experiments were conducted. The action of the other muscles can be explained in terms of the primary deformation caused by the strongly-contracting genioglossus. The transversis and superior longitudinal are also active to prevent the lateral elongation of the superior surface and antero-inferior motion of the tongue tip respectively due to the shortening of the genioglossus. The hyoglossus further assists by lowering the posterior region of the tongue in the direction of the mouth floor, and the inferior longitudinal, in conjunction with its superior counterpart, shortens the blade length. The influence of the other muscles appears minimal in this case. As it has been demonstrated that the genioglossus exhibits the greatest response to the loads, we will concentrate our analysis on its behaviour under several differing conditions.

The result of the contraction which opposes the loads is that the stress distributions present within the tongue differ significantly as the conditions change. Visualized in figure 12 are the primary stresses induced in the tongue body and the contractile stresses in the genioglossal muscle fibres that are working to prevent its motion. The resulting stresses are largest at the root of the genioglossus, where muscle contraction occurs near the mandible fixture point. In addition to being the area of greatest constraint, it supports most of the weight of the tongue when in the supine orientation. The greatest contractile stresses generated in the central region of the posterior genioglossus as the fibre conditions are favourable (there exists only mild extension at this location) and its fibre volume fraction is greatest. However, the region of the fibres that work most effectively are actually present in the vicinity of the tongue surface and in the medial part of the genioglossus. Since the bulk of the tongue is largely free to deform, the stresses generated in the tongue volume are relatively low.

Illustrated in figure 13 is the influence that posture has on the active response of the genioglossus. These results align with observations provided by Remmers et al. [1978], Akahoshi et al. [2001], Malhotra et al. [2002b] in that the predicted response of the genioglossus is linear with respect to the epiglottal pressure. However, the zero-pressure response is dictated by the posture and this quantifies the degree of muscle contraction required to resist the force of gravity. The crossing-value is in both cases non-linear with respect to the angle of inclination, but for the posterior part of the genioglossus is linear with respect to the angle cosine (the component of the gravitational force in the posterior direction). Furthermore, it can be observed that the angle-response relationship for the poster and medial genioglossus differ significantly. This is due to the degree to which the muscle fibres and gravitational force align, with the posterior fibres in very good alignment with the gravitational forces in the supine orientation.

The medial part is best suited to prevent the superior surface of the tongue from lifting towards the palate. As the angle of inclination increases towards the upright position, the forces that induce this motion become less effective, thereby reducing the necessity for its activation.

The pressure drop through the airway is related to its cross-sectional area. In changing the peak epiglottal pressure, we simulate cases where the cross-sectional area of the airway differs. Shown in figure 14 is the result of such a change, where the minimum pressure experienced in the airway is decreased from  $-200Pa$  to  $-1kPa$ . As can be expected, the response from the genioglossus continues to follow the loading pattern closely, and these muscles contract with greater strength as the pressure load increases. In all cases, the degree to which muscles are contracted at zero load were comparable. Although in this instance the loading rate changes as the period over which the load is applied remains constant, this did not significantly affect the linear pressure-contraction response of these muscles. The nature of the response by the medial genioglossus was more erratic than that of the posterior part, as it is more heavily influenced by the contraction of the surrounding muscles.

In figure 15 we present the difference in response of the genioglossus under conditions which simulate breathing through the mouth and nose. Clearly visible is a marked difference in response of the medial and posterior genioglossus for each case. Compared to the base case of oral inhalation which we have presented thus far, nasal inhalation requires little change in effort for both muscles as the airway pressure drops.

Relaxation was observed in the posterior component, while only slight stiffening of the medial component was required. This is because the pressure load on the tongue is nearly evenly distributed, resulting in little force, other than gravitationally derived, acting on the tongue. However, when the oral cavity

is sealed off, the medial component remains fairly inactive while the posterior portion is required to generate substantial forces to overcome the load which would otherwise cause retroglossal movement. This demonstrates quite clearly the roles of these two muscles; the posterior genioglossus acts to prevent posterior motion of the tongue, while the medial part prevents only superior motion. The former is produced by gravitational loads aligned in the antero-posterior direction and pressure on the rear of the tongue, while the “lifting” loads are produced by pressure loads of the superior surface of the tongue and the tendency for the tongue to twist around the thyroid-fixture when gravitational forces align in the posterior direction.

During an OSA event, brief instances of heavy breathing may occur. In such events, the airway dilators are required to respond more rapidly to changing loads. Figure 16 illustrates the change in the response as the rate at which inhalation occurs is increased. Due to the force-velocity relationship, there is a decrease in efficiency of the muscles as the rate at which contraction occurs is increased. Therefore, a more intense neurological signal is required to overcome the inefficiency and produce sufficient muscle shortening and force. For the posterior genioglossus, the relationship between inhalation-rate and peak muscle response is somewhat linear; however, the medial component does not have as clear a dependence.

A first approximation of the effect of the constitution of the muscle has been constructed. To perform this evaluation, we altered the relative fractions of the muscle matrix, adipose tissue and composite fibres. As can be seen in figure 17, an increase in the matrix/adipose contribution (presented as a reduction in the total fibre volume fraction) resulted in the necessity for greater muscle contraction to overcome the applied loads. Note that both the zero- and maximal-pressure response has changed. The increase in contraction effort

scaled proportionally to the decrease in fibre content. This result suggests that the change in physiology that occurs as the overall body fat percentage increases necessitates a change in the neurological response required to prevent tongue displacement due to both gravitational and pressure loads.

## 5 Conclusion

We have described a mathematical and computational model which represents the anatomy of the human tongue and surrounding tissues. The methodology of model construction, from raw imaging data to a macro- and micro-geometry suitable for analysis using the FEM has been detailed, and simplifications of the gross-anatomical structures have been listed. Coupled with this is the description of a phenomenological model which captures and simulates the functioning of active skeletal muscle, of which much of the tongue is composed.

A brief description of a model which mimics the proprioceptive responses of the nervous system has been provided, and it has been demonstrated that such a model is capable of preventing motion induced by *a priori* unknown forces in this complex dynamical system.

Collectively, this model has been used to study the muscular response of the tongue during conditions that simulate both oral and nasal inhalation. It has been demonstrated that the response of the genioglossus is qualitatively similar to that determined through experimental techniques. Furthermore, we have provided some insights into the stress-distribution developed within the tongue. Additionally, the synergistic activation of the other muscles of the tongue has been illustrated, and described how they behave in conjunction with the genioglossus. Following on from this, studies were performed under differing physiological and environmental conditions to describe how the genioglossus responds differently as the conditions change.

It has been shown that changing almost any aspect of the breathing or physiological conditions invokes a significant change in the response of the airway dilators.

## **6 Acknowledgements**

The authors acknowledge and thank Dr Andrew McBride, Mr Yaseen Kajee, Dr Yougan Saman and Dr Indresan Govender for their discussions and contributions towards this work. Funding for this work is provided by the National Research Foundation through the South African Research Chair for Computational Mechanics, and the University of Cape Town.

## **7 Conflict of interest**

The authors have no conflict of interest to declare.

## References

- S. Abd-El-Malek. Observations on the morphology of the human tongue. *Journal of Anatomy*, 73:201–210, 1939.
- A. M. R. Agur and A. F. Dalley. *Grant’s Atlas of Anatomy*. Lippincott Williams & Wilkins, 351 West Camden Street, Baltimore, Maryland, 21201, USA, 11 edition, 2005.
- T. Akahoshi, D. White, J. K. Edwards, J. Beauregard, and S. A. Shea. Phasic mechanoreceptor stimuli can induce phasic activation of upper airway muscles in humans. *Journal of Physiology*, 531.3:677–691, 2001.
- I. Ayappa and D. M. Rapoport. The upper airway in sleep: physiology of the pharynx. *Sleep Medicine Reviews*, 7:9–33, 2003.
- F. Baaijens, C. Bouten, and N. Driessen. Modeling collagen remodeling. *Journal of Biomechanics*, 43:166–175, 2010.
- W. Bangerth, R. Hartmann, and G. Kanschat. deal.II — a general-purpose object-oriented finite element library. *ACM Transactions on Mathematical Software*, 33(4), 2007. doi: 10.1145/1268776.1268779. Article 24, 27 pages.
- J. M . Battagel, A. Johal, A-M. Smith, and B. Kotecha. Postural variation in oropharyngeal dimensions in subjects with sleep disordered breathing: a cephalometric study. *European Journal of Orthodontics*, 24:263–276, 2002.
- M. J. Brennick, S. Pickup, L. Dougherty, J. R. Cater, and S. T. Kuna. Pharyngeal airway wall mechanics using tagged magnetic resonance imaging during medial hypoglossal nerve stimulation in rats. *Journal of Physiology*, 561:597–610, 2004. doi: 10.1113/jphysiol.2004.073502.

- S. Buchaillard and P. Perrier. A biomechanical model of cardinal vowel production: Muscle activations and the impact of gravity on tongue positioning. *Acoustical Society of America*, 126:2033–2051, 2009.
- N. J. Buchner, B. M. Sanner, J. Borgel, and L. C. Rump. Continuous positive airway pressure treatment of mild to moderate obstructive sleep apnea reduces cardiovascular risk. *American Journal of Respiratory and Critical Care Medicine*, 176:1274–1280, 2007.
- M. Butt, G. Dwivedi, O. Khair, and G. Y. H. Lip. Obstructive sleep apnea and cardiovascular disease. *International Journal of Cardiology*, 179:7–16, 2010.
- P. Caballero, R. Alvarez-Sala, F. García-Río, C. Prados, M. A. Hernán, J. Villamor, and J. L. Alvarez-Sala. Ct in the evaluation of the upper airway in healthy subjects and in patients with obstructive sleep apnea syndrome. *Chest*, 113:111–116, 1998. doi: 10.1378/chest.113.1.111.
- M. Carrera, F. Barbe, J. Sauleda, M. Tomas, C. Gomez, C. Santosz, and A. G. N. Agustí. Effects of obesity upon genioglossus structure and function in obstructive sleep apnoea. *European Respiratory Journal*, 23:425–429, 2004. doi: 10.1183/09031936.04.00099404.
- S. Cheng, J. E. Butler, S. C. Gandevia, and L. E. Bilston. Movement of the tongue during normal breathing in awake healthy humans. *The Journal of Physiology*, 586:4283–4294, 2008.
- G. T. Clark. Mandibular advancement devices and sleep disordered breathing. *Sleep Medicine Reviews*, 3:163–174, 1998.
- G. K. Cole, A. J. van den Bogert, W. Herzog, and K. G. M. Gerritsen. Modelling of force production in skeletal muscle undergoing stretch. *Journal of Biomechanics*, 29(8):1091–1104, August 1996. URL

<http://www.sciencedirect.com/science/article/B6T82-3W0NDMG-F/1/487c0be697b4c6b14cd1c6b8cac7271f>.

- R. Cooke, H. White, and E. Pate. A model of the release of myosin heads from actin in rapidly contracting muscle fibers. *Biophysical Journal*, 66:778–788, 1994.
- F. Dalmasso and R. Prota. Snoring: analysis, measurement, clinical implications and applications. *European Respiratory Journal*, 9:146–159, 1996.
- J. Dang and K. Honda. A physiological articulatory model for simulating speech production process. *Acoustical Science and Technology*, 22:415–425, 2001.
- J. Dang and K. Honda. Construction and control of a physiological articulatory model. *Journal of the Acoustical Society of America*, 115:853–870, 2004.
- D. D’Aulignac, J. A. C. Martins, E. B. Pires, T. Mascharenhas, and R. M. Natal Jorge. A shell finite element model of the pelvic floor muscles. *Computer Methods in Biomechanics and Biomedical Engineering*, 8:339–347, 2005.
- T. M. Davidson. Sleep medicine for surgeons. *Laryngoscope*, 118(5):915–931, May 2008. doi: 10.1097/MLG.0b013e3181670fc4. URL <http://dx.doi.org/10.1097/MLG.0b013e3181670fc4>.
- D.V. Davies, editor. *Gray’s Anatomy*. Longmans, Green & Co Ltd., 48 Grosvenor Street, London, Uk, 34th edition, 1967.
- S. dos Reis Zinsly, L. C. de Moraes, P. de Moura, and W. Ursi. Assessment of pharyngeal airway space using cone-beam computed tomography. *Dental press journal of orthodontics*, 15:150–158, 2010.
- N. J. B. Driessen, C. V. C. Bouten, and F. P. T. Baaijens. A structural constitutive model for collagenous cardiovascular tissues incorporating the

- angular fiber distribution. *Journal of Biomechanical Engineering*, 127: 494–503, 2005.
- A. Erdemir, M. L. Viveiros, J. S. Ulbrecht, and P. R. Cavanagh. An inverse finite-element model of heel-pad indentation. *Journal of Biomechanics*, 39: 1279–1286, 2006.
- Q. Fang, S. Fujita, X. Lu, and J. Dang. A model-based investigation of activations of the tongue muscles in vowel production. *Acoustical Science and Technology*, 30:277–287, 2009.
- M. S. Farvid, T. W. Ng, D. C. Chan, P. H. Barrett, and G. F. Watts. Association of adiponectin and resistin with adipose tissue compartments, insulin resistance and dyslipidaemia. *Diabetes, Obesity and Metabolism*, 7: 406–413, 2005.
- R. B. Fogel, A. Malhotra, and D. P. White. Pathophysiology of obstructive sleep apnoea/hypopnoea syndrome. *Thorax*, 59:159–163, 2004. doi: 10.1136/thx.2003.015859.
- S. I. Fox. *Human Physiology*. McGraw-Hill, ninth edition, 2006.
- U. Froberg, R. J. Naples, and D. L. Jones. Cephalometric comparison of characteristics in chronically snoring patients with and without sleep apnea syndrome. *Oral Surgery Oral Medicine Oral Pathology*, 80:28–33, 1995.
- S. Fujita, J. Dang, N. Suzuki, and K. Honda. A computational tongue model and its clinical application. *Oral Science International*, 109:97–109, 2007.
- Y. C. Fung. *Biomechanics: Mechanical Properties of Living Tissues Second Edition*. Springer, 233 Spring Street, New York, Ny 10013, USA, 1993.
- T. A. Gaige, T. Benner, R. Wang, V. J. Wedeen, and R. J. Gilbert. Three dimensional myoarchitecture of the human tongue determined in vivo by

- diffusion tensor imaging with tractography. *Journal of Magnetic Resonance Imaging*, 26:650–661, 2007.
- J-M. Gérard, R. Wilhelms-Tricarico, P. Perrier, and Y. Payan. A 3d dynamical biomechanical tongue model to study speech motor control. *Recent Research Developments in Biomechanics*, 1:49–63, 2003.
- D. E. Goldberg. *Genetic algorithms in search, optimization and machine learning*. Addison-Wesley Longman, 1989.
- A. M. Gordon, A. F. Huxley, and F. J. Julian. Tension development in highly stretched vertebrate muscle fibres. *Journal of Physiology*, 184:143–169, 1966a.
- A. M. Gordon, A. F. Huxley, and F. J. Julian. The variation in isometric tension with sarcomere length in vertebrate muscle fibres. *Journal of Physiology*, 184:170–192, 1966b.
- M. Hagopian. Contraction bands at short sarcomere length in chick muscle. *Journal of Cell Biology*, 47:790–796, 1970.
- E. P. P. M. Hamans, E. A. Van Marck, W. A. De Backer, W. Creten, and P. H. Van de Heyning. Morphometric analysis of the uvula in patients with sleep-related breathing disorders. *European Archives of Oto-Rhino-Laryngology*, 257:232–236, 2000. ISSN 0937-4477. URL <http://dx.doi.org/10.1007/s004050050229>. 10.1007/s004050050229.
- R. L. Haupt and S. E. Haupt. *Practical Genetic Algorithms*. John Wiley & Sons Inc., 2<sup>nd</sup> edition, 2004.
- M. A. Heroux, R. A. Bartlett, V. E. Howle, R. J. Hoekstra, J. J. Hu, T. G. Kolda, R. B. Lehoucq, K. R. Long, R. P. Pawlowski, E. T. Phipps, A. G. Salinger, H. K. Thornquist, R. S. Tuminaro, J. M. Willenbring, A. Williams,

- and K. S. Stanley. An overview of the trilos project. *ACM Trans. Math. Softw.*, 31(3):397–423, 2005.
- W. Herzog and R. Ait-Haddou. Considerations on muscle contraction. *Journal of Electromyography and Kinesiology*, 12:425–433, 2002.
- A. V. Hill. The heat of shortening and the dynamic constants of muscle. *Proceedings of the Royal Society of London, Series B*, 126:136–195, 1938.
- A. V. Hill. The mechanics of active muscle. *Proceedings of the Royal Society of London. Series B.*, 141:104–117, 1953.
- G. A. Holtzapfel, T. C. Gasser, and R. W. Ogden. A new constitutive framework for arterial wall mechanics and a comparative study of material models. *Journal of Elasticity*, 61:1–48, 2000.
- L. Hu, X. Xu, Y. Gong, X. Fan, L. Wang, J. Zhang, and Y. Zeng. Percutaneous biphasic electrical stimulation for treatment of obstructive sleep apnea syndrome. *IEEE Transactions on Biomedical Engineering*, 55:181–187, 2008.
- Y. Huang, A. Malhotra, and D. P. White. Computational simulation of human upper airway collapse using a pressure-/state-dependent model of genioglossal muscle contraction under laminar flow conditions. *J Appl Physiol*, 99(3):1138–1148, September 2005a. URL <http://jap.physiology.org/cgi/content/abstract/99/3/1138>.
- Y. Huang, D. P. White, and A. Malhotra. The impact of anatomic manipulations on pharyngeal collapse: Results from a computational model of the normal human upper airway. *Chest*, 128(3):1324–1330, September 2005b. URL <http://www.chestjournal.org/cgi/content/abstract/128/3/1324>.
- Y. Huang, D. P. White, and A. Malhotra. Use of computational modeling

- to predict responses to upper airway surgery in obstructive sleep apnea. *Laryngoscope*, 117:648–653, 2007.
- T. J. Hughes. *The Finite Element Method: Linear Static and Dynamic Finite Element Analysis*. Dover Publications Inc., 2000.
- I. A. Humbert, S. B. Reeder, E. J. Porcaro, S. A. Kays, J. H. Brittain, and J. Robbins. Simultaneous estimation of tongue volume and fat fraction using ideal-fse. *Journal of Magnetic Resonance Imaging*, 28:504–508, 2008.
- J. D. Humphrey and F. C. P. Yin. On constitutive relations and finite deformations of passive cardiac tissue: I. a pseudostrain-energy function. *Journal of Biomechanical Engineering*, 109:298–304, 1987.
- J. D. Humphrey, R. K. Strumpf, and F. C. P. Yin. Determination of a constitutive relation for passive myocardium: I. a new functional form. *Journal of Biomechanical Engineering*, 112:333 – 339, 1990.
- A. F. Huxley. Review lecture: Muscle contraction. *Journal of Physiology*, 243: 1 – 43, 1974.
- Ansys Inc. <http://www.ansys.com/products/icemcfd.asp>, December 2010.
- T. Ingman, T. Nieminen, and K. Hurmerinta. Cephalometric comparison of pharyngeal changes in subjects with upper airway resistance syndrome or obstructive sleep apnoea in upright and supine positions. *European Journal of Orthodontics*, 26:321–326, 2004.
- Intel(R) Threading Building Blocks: Reference Manual*. Intel Corporation, 2011.  
URL <http://software.intel.com/sites/products/documentation/hpc/tbb/referencev3.pdf>.

- S. Isono, J. E. Remmers, A. Tanaka, Y. Sho, J. Sato, and T. Nishino. Anatomy of pharynx in patients with obstructive sleep apnea and in normal subjects. *Journal of Applied Physiology*, 82:1319–1326, 1997.
- S. Isono, A. Tanaka, and T. Nishino. Effects of tongue electrical stimulation on pharyngeal mechanics in anaesthetized patients with obstructive sleep apnoea. *European Respiratory Journal*, 14:1258–1265, 1999.
- S. Isono, A. Tanaka, and T. Nishino. Dynamic interaction between the tongue and soft palate during obstructive apnea in anesthetized patients with sleep-disordered breathing. *Journal of Applied Physiology*, 95:2257–2264, 2003. doi: 10.1152/japplphysiol.00402.2003.
- T. Johansson, P. Meier, and R. Blickhan. A finite-element model for the mechanical analysis of skeletal muscles. *Journal of Theoretical Biology*, 206:131–149, 2000. doi: 10.1006/jtbi.2000.2109.
- N. T. Johnson and J. Chinn. Uvulopalatopharyngoplasty and inferior sagittal mandibular osteotomy with genioglossus advancement for treatment of obstructive sleep apnea. *Chest*, 105:278–283, 1994.
- Y. Kaje, J-P. V. Pelteret, and B. D. Reddy. The biomechanics of the human tongue. *International Journal for Numerical Methods in Biomedical Engineering*, 29:492–514, 2013. doi: 10.1002/cnm.2531.
- G. Karypis and V. Kumar. MeTis: Unstructured Graph Partitioning and Sparse Matrix Ordering System, Version 4.0, 2009. URL <http://www.cs.umn.edu/~metis>. Last visited: July 2012.
- L. P. Li, J. Soulhat, M. D. Buschmann, and A. Shirazi-Adl. Nonlinear analysis of cartilage in unconfined ramp compression using a fibril reinforced poroelastic model. *Clinical Biomechanics*, 14:673–682, 1999.

- R. L. Lieber. *Skeletal Muscle Structure, Function and Plasticity: The Physiological Basis of Rehabilitation*. Lippincott, Williams and Wilkins, 351 West Camden Street, Baltimore, Maryland, 21201, USA, 2002.
- R. L. Lieber, E. Runesson, F. Einarsson, and J. Friden. Inferior mechanical properties of spastic muscle bundles due to hypertrophic but compromised extracellular matrix material. *Muscle Nerve*, 28:464–471, 2003.
- J. E. Lloyd, I. Stavness, and S. Fels. Artisynth: A fast interactive biomechanical modeling toolkit combining multibody and finite element simulation. *Soft Tissue Biomechanical Modeling for Computer Assisted Surgery*, 11:355–394, 2012. doi: 10.1007/8415\_2012\_126.
- M. Madani. Surgical treatment of snoring and mild obstructive sleep apnea. *Oral & Maxillofacial Surgery Clinics of North America*, 14:333–350, 2002.
- A. Malhotra and D. P. White. Obstructive sleep apnoea. *The Lancet*, 360: 237–245, July 2002.
- A. Malhotra, G. Pillar, R. B. Fogel, J. Beauregard, J. K. Edwards, D. I. Slamowitz, S. A. Shea, and D. P. White. Genioglossal but not palatal muscle activity relates closely to pharyngeal pressure. *American Journal of Respiratory and Critical Care Medicine*, 162:10581062, 2000.
- A. Malhotra, Y. Huang, R. B. Fogel, G. Pillar, J. K. Edwards, R. Kikinis, S. H. Loring, and D. P. White. The male predisposition to pharyngeal collapse: Importance of airway length. *American Journal of Respiratory and Critical Care Medicine*, 66:1388–1395, 2002a.
- A. Malhotra, G. Pillar, R. B. Fogel, J. K. Edwards, N. Ayas, T. Akahoshi, D. Hess, and D. P. White. Pharyngeal pressure and flow effects on genioglossus

- activation in normal subjects. *American Journal of Respiratory and Critical Care Medicine*, 165:71–77, 2002b.
- J. A. C. Martins, E. B. Pires, R. Salvado, and P. B. Dinis. A numerical model of passive and active behaviour of skeletal muscles. *Computer Methods in Applied Mechanics and Engineering*, 151:419–433, 1998.
- J. A. C. Martins, M. P. M. Pato, and E. B. Pires. A finite element model of skeletal muscles. *Virtual and Physical Prototyping*, 1(1):159–170, September 2006.
- P. Mayer, J-L. Pépin, G. Bettenga, D. Veale, G. Ferretti, C. Deschaux, and P. Lévy. Relationship between body mass index, age and upper airway measurements in snorers and sleep apnoea patients. *European Respiratory Journal*, 9:1801–1809, 1996.
- W. T. McNicholas. The nose and osa: variable nasal obstruction may be more important in pathophysiology than fixed obstruction. *European Respiratory Journal*, 32:3–8, 2008.
- C. Miehe. Aspects of the formulation and finite strain element implementation of large strain isotropic elasticity. *International Journal for Numerical Methods in Engineering*, 37:1981–2004, 1994.
- S. M. Mijailovich, J. J. Fredberg, and J. P. Butler. On the theory of muscle contraction: Filament extensibility and the development of isometric force and stiffness. *Biophysical Journal*, 71:1475–1484, 1996.
- J. L. Miller, K. L. Watkin, and M. Y. Chen. Muscle, adipose, and connective tissue variations in intrinsic musculature of the adult human tongue. *Journal of Speech, Language, and Hearing Research*, 45:51–65, 2002.

- R. P. Millman, C. L. Rosenberg, C. C. Carlisle, N. R. Kramer, D. M. Kahn, and A. E. Bonitati. The efficacy of oral appliances in the treatment of persistent sleep apnea after uvulopalatopharyngoplasty. *Chest*, 113:992–996, 1998.
- Melanie Mitchell. *An Introduction to Genetic Algorithms*. MIT Press, 55 Hayward Street, Cambridge, Massachusetts 02142-1493, USA, 1999.
- K. Miyawaki, H. Hirose, T. Ushijima, and M. Sawashima. A preliminary report on the electromyographic study of the activity of lingual muscles. *Annual Bulletin RILP*, 9:91–106, 1975.
- M. E. Mortley. *The Development and Disorders of Speech in Childhood*. Churchill Livingstone, third edition, 1972.
- N. Nashi, S. Kang, G. C. Barkdull, J. Lucas, and T. M. Davidson. Lingual fat at autopsy. *Laryngoscope*, 117:1467–1473, 2007.
- Materialise NV. <http://www.materialise.com/mimics>, December 2010.
- A. Oliven, N. Tov, L. Geitini, U. Steinfeld, R. Oliven, A. R. Schwartz, and M. Odeh. Effect of genioglossus contraction on pharyngeal lumen and airflow in sleep apnoea patients. *European Respiratory Journal*, 30:748–758, 2007.
- T. Ono, A. A. Lowe, K. A. Ferguson, E-K Pae, and J. A. Fleetham. The effect of the tongue retaining device on awake genioglossus muscle activity in patients with obstructive sleep apnea. *American Journal of Orthodontics and Dentofacial Orthopedics*, 110:28–35, 1996.
- M. M. Ozbek, K. Miyamoto, A. Lowe, and J. A. Fleetham. Natural head posture, upper airway morphology and obstructive sleep apnoea severity in adults. *European Journal of Orthodontics*, 20:133–143, 1998.

- E-K. Pae, A. A. Lowe, and J. A. Fleetham. A role of pharyngeal length in obstructive sleep apnea patients. *American Journal of Orthodontics and Dentofacial Orthopedics*, 111:12–17, 1997.
- M. G. Pandy. Computer modelling and simulation of human movement. *Annual Review of Biomedical Engineering*, 3:245 – 273, 2001.
- M. G. Pandy, F. E. Zajac, E. Sim, and W. S. Levine. An optimal control model for maximum-height human jumping. *Journal of Biomechanics*, 23: 1185–1198, 1990.
- J-P. V. Pelteret and B. D. Reddy. Computational model of soft tissues in the human upper airway. *International Journal for Numerical Methods in Biomedical Engineering*, 28:111–132, 2012. doi: 10.1002/cnm.1487.
- P. Perrier, Y. Payan, M. Zandipour, and J. Perkell. Influences of tongue biomechanics on speech movements during the production of velar stop consonants: A modeling study. *Journal of the Acoustical Society of America*, 114:1582–1599, 2003.
- C. S. Peskin. *Mathematical Aspects of Heart Physiology*. Courant Institute of Mathematical Sciences, 1975.
- D.R. Peterson and J.D. Bronzino. *Biomechanics: Principles and Applications*. CRC Press, 6000 Broken Sound Parkway NW, Suite 300, Boca Raton, Florida 33487-2742, USA, 2008.
- R. Pierce, D. White, A. Malhotra, J.K. Edwards, D. Kleverlaan, L. Palmer, and J. Trinder. Upper airway collapsibility, dilator muscle activation and resistance in sleep apnoea. *European Respiratory Journal*, pages 345–353, 2007.

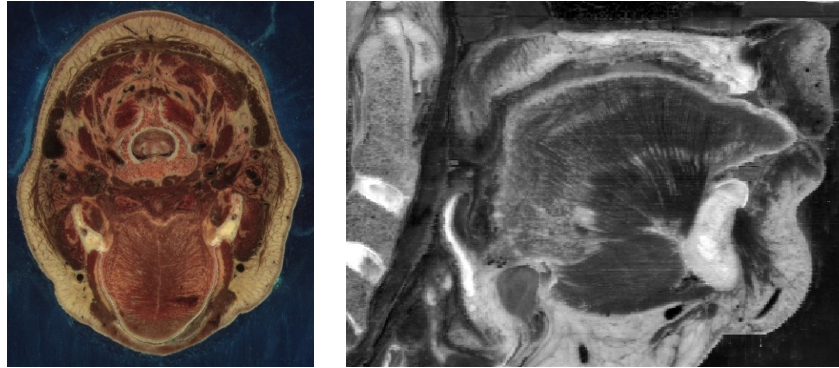
- M. Rappai, N. Collop, K. Kemp, and R. deShazo. The nose and sleep-disordered breathing: What we know and what we do not know. *Chest*, 124:2309–2323, 2003.
- D. E. Rassier, W. Herzog, J. Wakeling, and D. A. Syme. Stretch-induced, steady-state force enhancement in single skeletal muscle fibers exceeds the isometric force at optimum fiber length. *Journal of Biomechanics*, 36:1309–1316, 2003.
- D. T. Reilly and A. H. Burstein. The mechanical properties of cortical bone. *The Journal of Bone and Joint Surgery*, 56:1001–1022, 1974.
- J. E. Remmers, W. J. de Groot, E. K. Sauerland, and A. M. Anch. Pathogenesis of upper airway occlusion during sleep. *Journal of Applied Physiology*, 44:931–938, 1978.
- I. Rubinstein, A. S. Slutsky, N. Zamel, and Hoffstein. V. Paradoxical glottic narrowing in patients with severe obstructive sleep apnea. *Journal of Clinical Investigation*, 81:1051–1055, 1988.
- C. M. Ryan and T. D. Bradley. Pathogenesis of obstructive sleep apnea. *Journal of Applied Physiology*, 99:2440–2450, 2005.
- C.F. Ryan, L. L. Love, D. Peat, J. A. Fleetham, and A. A. Lowe. Mandibular advancement oral appliance therapy for obstructive sleep apnoea: effect on awake calibre of the velopharynx. *Thorax*, 24:972–977, 1999.
- V. Sanguineti, R. Laboissiere, and D. Ostry. A dynamic biomechanical model for neural control of speech production. *Journal of the Acoustical Society of America*, 103:1615–1627, 1998.
- R. J. Schwab, M. Pasirstein, R. Pierson, A. Mackley, R. Hachadoorian, R. Arens, G. Maislin, and A. I. Pack. Identification of upper airway anatomic risk factors

- for obstructive sleep apnea with volumetric magnetic resonance imaging. *American Journal of Respiratory and Critical Care Medicine*, 168:522–530, 2003.
- Y. Segal, A. Malhotra, and G. Pillar. Upper airway length may be associated with the severity of obstructive sleep apnea syndrome. *Sleep Breath*, 12: 311–316, 2008.
- H. Shinagawa, A. E. Murano, J. Zhuo, B. Landman, R. P. Gullapalli, J. L. Prince, and M. Stone. Tongue muscle fiber tracking during rest and tongue protrusion with oral appliances: A preliminary study with diffusion tensor imaging. *Acoustical Science and Technology*, 29:291–294, 2008.
- J. C. Simo and R. L. Taylor. Quasi-incompressible finite elasticity in principal stretches. Continuum basis and numerical algorithms. *Computer Methods in Applied Mechanics and Engineering*, 85:273–310, 1991.
- J. C. Simo, R. L. Taylor, and K. S. Pister. Variational and projection methods for the volume constraint in finite deformation elasto-plasticity. *Computer Methods in Applied Mechanics and Engineering*, 51:177–208, 1985.
- A. J. Sokoloff. Activity of tongue muscles during respiration: it takes a village? *Journal of Applied Physiology*, 96:438–439, 2004. doi: 10.1152/jappphysiol.01079.2003.
- V. Spitzer, M. J. Ackerman, A. L. Scherzinger, and Whitlock D. The visible human male: A technical report. *Journal of the American Medical Informatics Association*, 3:118–130, 1996.
- P. Stal, S. Marklund, L. E. Thornell, R. De Paul, and P. O. Eriksson. Fibre composition of human intrinsic tongue muscles. *Cells Tissues Organs*, 173: 147–161, 2003.

- M. L. Stanchina, A. Malhotra, R. B. Fogel, N. Ayas, J. K. Edwards, K. Schory, and D. P. White. Genioglossus muscle responsiveness to chemical and mechanical stimuli during nonrapid eye movement sleep. *American Journal of Respiratory and Critical Care Medicine*, 165:945–949, 2002.
- I. Stavness, J. E. Lloyd, Y. Payan, and S. Fels. Coupled hard-soft tissue simulation with contact and constraints applied to jaw-tongue-hyoid dynamics. *International Journal for Numerical Methods in Engineering*, 27: 367–390, 2011.
- Y. Tagaito, S. Isono, A. Tanaka, T. Ishikawa, and T. Nishino. Sitting posture decreases collapsibility of the passive pharynx in anesthetized paralyzed patients with obstructive sleep apnea. *Anesthesiology*, 113:812–818, 2010.
- H. Takemoto. Morphological analyses of the human tongue musculature for three-dimensional modeling. *Journal of Speech, Language, and Hearing Research*, 44:95–107, 2001.
- H. E. D. J. ter Keurs, T. Iwazumi, and G. H. Pollack. The sarcomere length-tension relation in skeletal muscle. *Journal of General Physiology*, 72:656–692, 1978.
- U.S. National Library of Medicine. The Visible Human Project ®. [http://www.nlm.nih.gov/research/visible/visible\\_human.html](http://www.nlm.nih.gov/research/visible/visible_human.html), August 2009. URL [http://www.nlm.nih.gov/research/visible/visible\\_human.html](http://www.nlm.nih.gov/research/visible/visible_human.html).
- C. A. Van Ee, A. L. Chasse, and B. S. Myers. Quantifying skeletal muscle properties in cadaveric test specimens: Effects of mechanical loading, postmortem time, and freezer storage. *Journal of Biomechanical Engineering*, 122:9–14, 2000.
- A. Van Hirtum, F. Chouly, A. Teul, and X. Payan, Y. and Pelorson. In-vitro

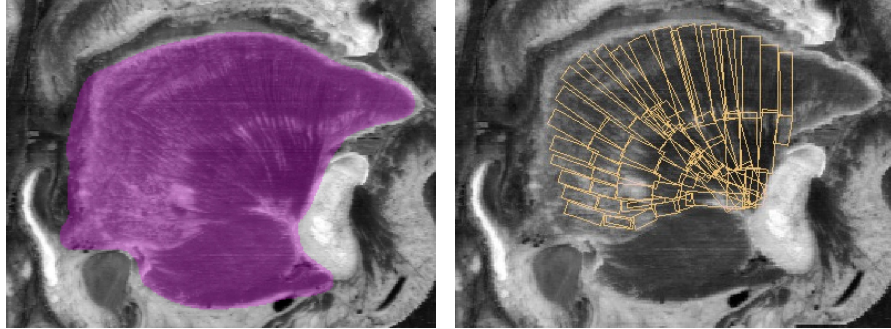
- study of pharyngeal pressure losses at the origin of obstructive sleep apnea. In *Engineering in Medicine and Biology Society, 2003. Proceedings of the 25th Annual International Conference of the IEEE*, Cancun, Mexico, September 2004.
- M. Van Loocke, C. G. Lyons, and C. K. Simms. A validated model of passive muscle in compression. *Journal of Biomechanics*, 39:2999–3009, 2006.
- C. H. G. A. van Oijen. *Mechanics and design of fiber-reinforced vascular prostheses*. PhD thesis, Technische Universiteit Eindhoven, 2003.
- M. Veldi, V. Vasar, T. Hion, M. Kull, and A. Vain. Ageing, soft-palate tone and sleep-related breathing disorders. *Clinical Physiology*, 21:358–364, 2001.
- F. Vogt, J. E. Lloyd, S. Buchaillard, P. Perrier, M. Chabanas, Y. Payan, and S. S. Fels. Efficient 3d finite element modeling of a muscle-activated tongue. In *ISBMS*, pages 19–28, 2006. doi: [http://dx.doi.org/10.1007/11790273\\_3](http://dx.doi.org/10.1007/11790273_3).
- W. Vos, A. J. De Backer, A. Devoldera, O. Vandervekena, S. Verhulsta, R. Salgadoc, P. Germonprea, B. Partoensb, F. Wuytsb, P. Parizelc, and W. A. De Backer. Correlation between severity of sleep apnea and upper airway morphology based on advanced anatomical and functional imaging. *Journal of Biomechanics*, 10:2207–2213, 2007. doi: 10.1016/j.jbiomech.2006.10.024.
- P. D. Waite. Obstructive sleep apnea: A review of the pathophysiology and surgical management. *Oral Surgery Oral Medicine Oral Pathology*, 85: 352–361, 1998.
- Matthew Wall. GALib: A C++ Library of Genetic Algorithm Components, July 2010. URL <http://lancet.mit.edu/ga/>. Version 2.4.7.
- D. P. White. The pathogenesis of obstructive sleep apnea: Advances in the past

- 100 years. *American Journal of Respiratory Cell and Molecular Biology*, 34: 1–6, 2006.
- R. Wilhelms-Tricarico. Physiological modeling of speech production: Methods for modeling soft-tissue articulators. *Journal of the Acoustical Society of America*, 97:3085–3098, 1995.
- W. O. Williams. Huxleys model of muscle contraction with compliance. *Journal of Elasticity*, 105:365–380, 2011.
- J. Z. Wu and W. Herzog. Modelling concentric contraction of muscle using an improved cross-bridge model. *Journal of Biomechanics*, 32:837–848, 1999.
- M. C. Wu, J. C. Han, O. Röhrle, W. Thorpe, and P. Nielsen. Using three-dimensional finite element models and principles of active muscle contraction to analyse the movement of the tongue. In *11th Australian International Conference on Speech Science & Technology*, pages 354–359. University of Auckland, Australasian Speech Science and Technology Association Inc, December 2006.
- G. I. Zahalak and S. Ma. Muscle activation and contraction: Constitutive relations based directly on cross-bridge kinetics. *Journal of Biomechanical Engineering*, 112:52–62, February 1990.



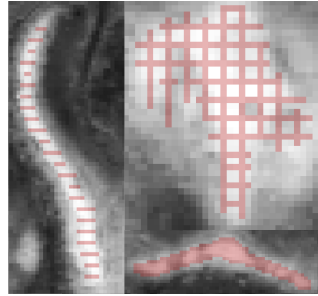
(a) Transverse section (original view)      (b) Coronal section (reconstructed view)

Figure 1: The buccal region of the female specimen of the VHP as viewed using commercial imaging software. The use of real-colour photography allowed for better small-feature visibility but differentiation of anatomical features was problematic.

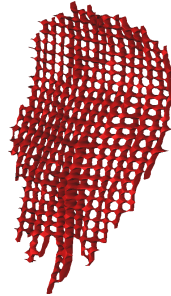


(a) Region selection for reconstruction of macro-histology (b) Region masking for muscle fibre definition

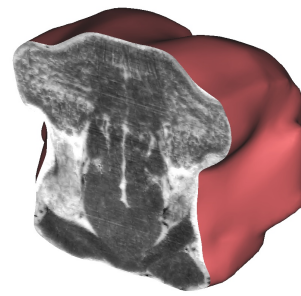
Figure 2: Process of definition of macro- and micro-scale information (sagittal viewpoint). Distinct large-scale anatomical parts are defined by separate masks, while collections of cylinders define the underlying histology.



(a) Layer masking of skeleton model



(b) Skeleton of anatomical part



(c) Transverse section through tongue volume

Figure 3: Volumetric data-sets of soft-tissue anatomy.

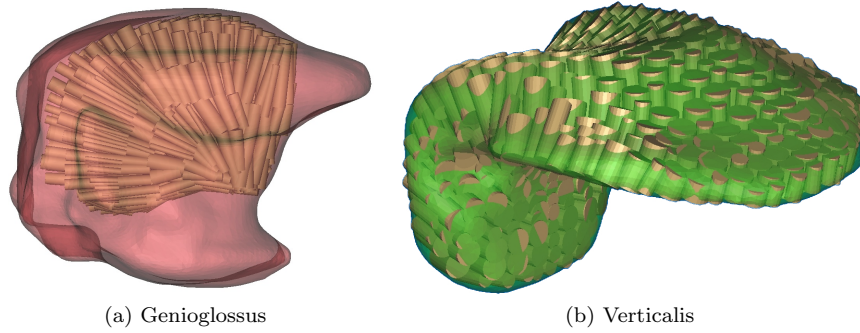


Figure 4: Directional data-sets of muscle micro-histology as defined within the imaging software. In figure 4b, a volumetric representation of the muscle, produced to locate its extents, is visible along with the directional data.

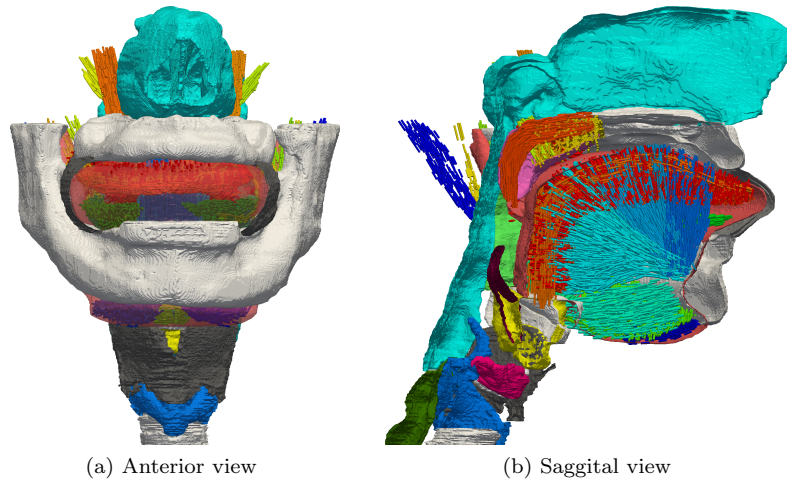


Figure 5: The completed reconstruction of the imaging data-set showing the upper-airway anatomy and microhistology. The unnatural positioning of the tongue is clearly visible.

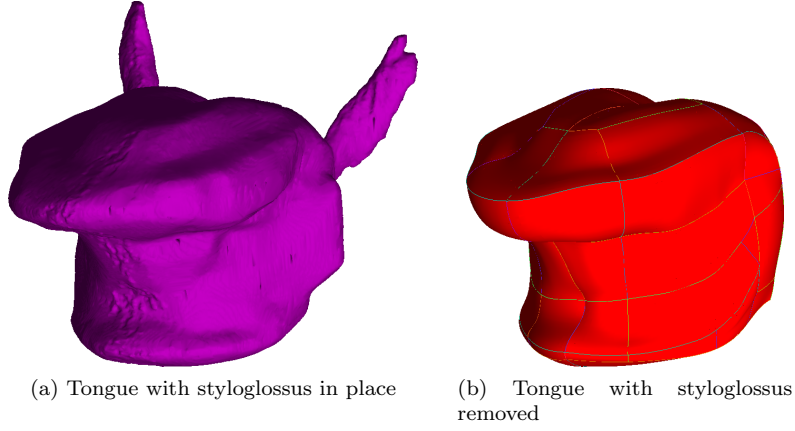


Figure 6: CAD reconstruction and feature removal for model simplification. The volumetric data for each part of the anatomy is re-represented as a set of smoothed surfaces.

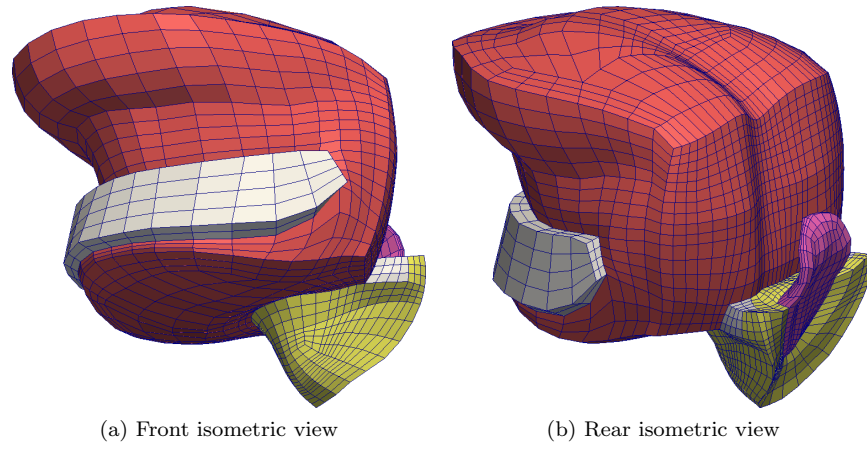
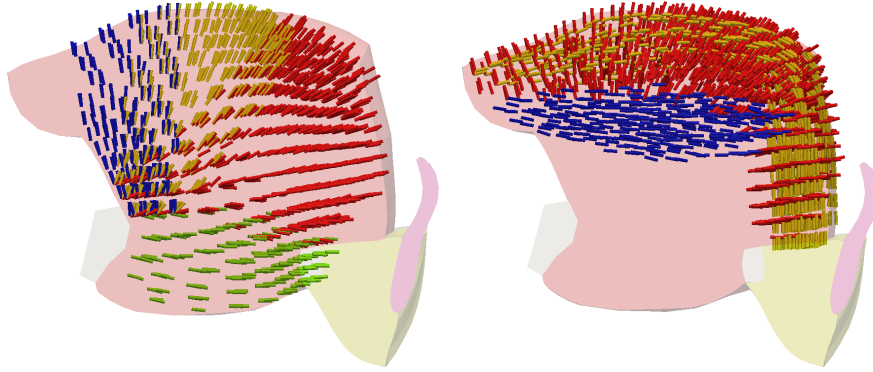
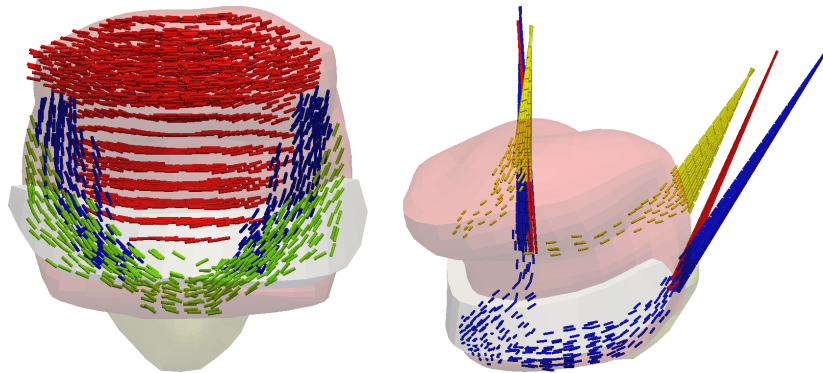


Figure 7: Final anatomical model of tongue and surrounding soft-tissues. Part of the mandible and hyoid are shown in grey, the tongue in pink, the epiglottal cartilage in magenta and adipose tissue in yellow.

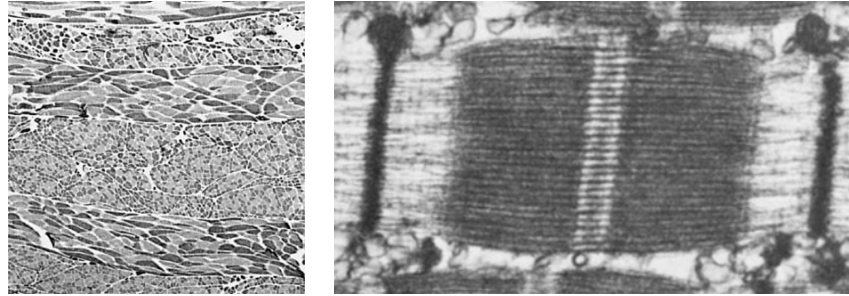


(a) Anterior (blue), medial (yellow) and (b) Inferior (blue) and superior (yellow) posterior (red) genioglossus; Geniohyoid longitudinal; Verticalis (red) (green)



(c) Hyoglossus (blue); Mylohyoid (green); Transversis (red) (d) Digastric (blue); Styloglossus (yellow); Stylohyoid (red)

Figure 8: Geometric description of the tongue musculature. Each cylinder within the tongue body represents the average directionality of eight fibres embedded within a computational cell.



(a) Cross-section of the verticalis situated in the middle-anterior region of the tongue [Stal et al., 2003] (b) Electron microscope image of a collection of sarcomeres from skeletal muscle [Hagopian, 1970]

Figure 9: Micro-histology of skeletal muscle fibres. Muscle fibres of varying orientation, as well as interstitial tissue, is clearly visible in figure 9a.

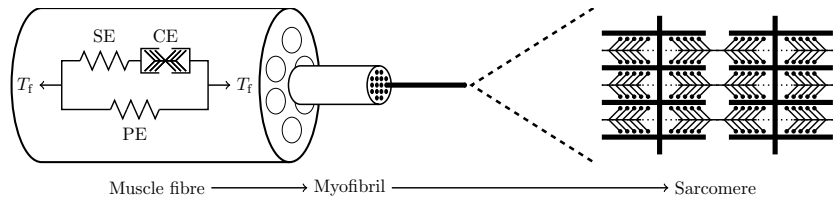


Figure 10: The Hill three-element model: A representative model of muscle micro-histology

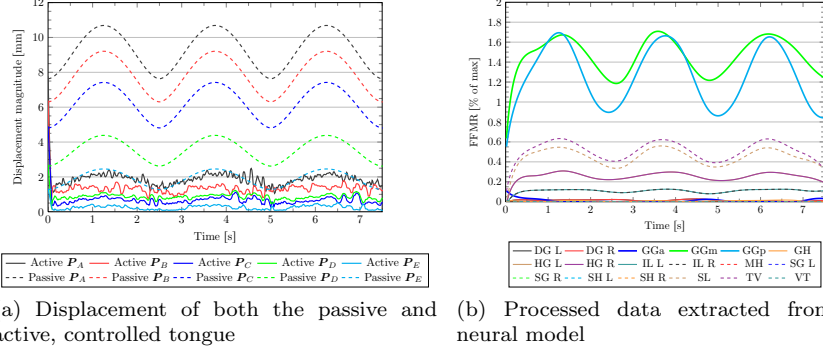


Figure 11: Strength of muscle contraction data predicted by neural model. Modelled posture: Supine. The location of the measured points, all on the mid-sagittal plane, are as follows:  $P_A$  – Tongue tip;  $P_B$  – Middle-superior surface of tongue;  $P_C$  – Upper-posterior surface of tongue, nearest the uvula;  $P_D$  – Middle-posterior surface of tongue;  $P_E$  – Tip of epiglottis

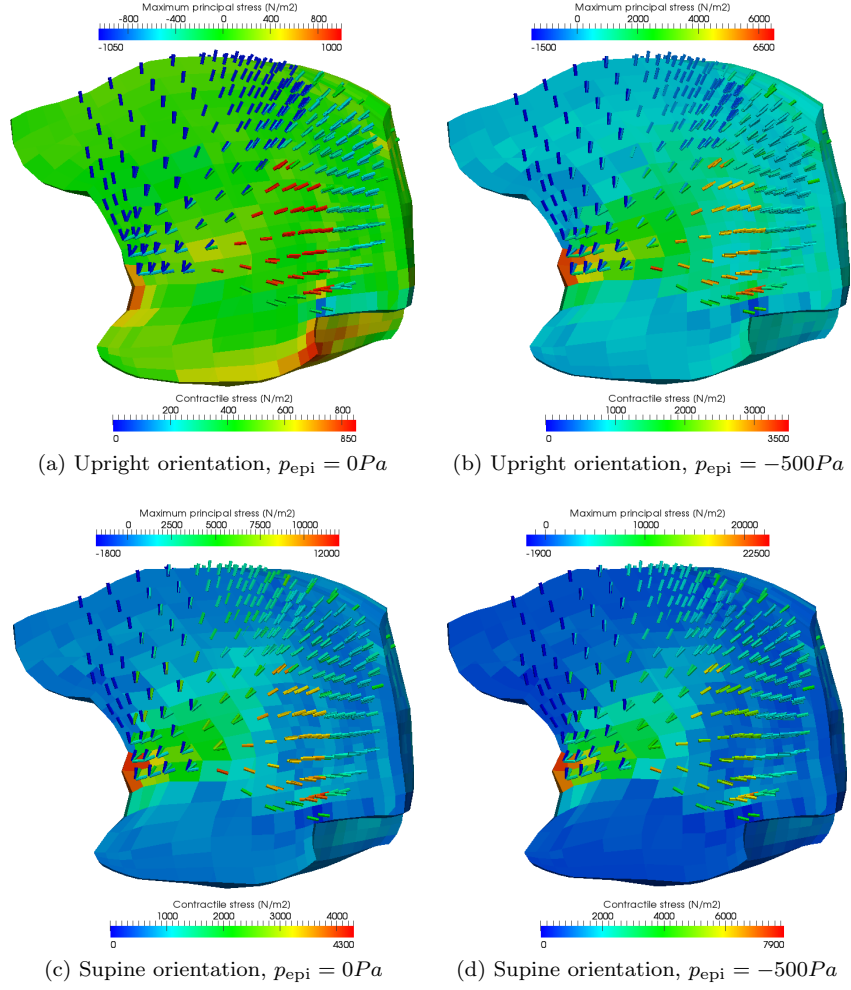


Figure 12: Stresses induced in the tongue due to gravitational and pressure forces (oral inhalation), as well as muscle activation

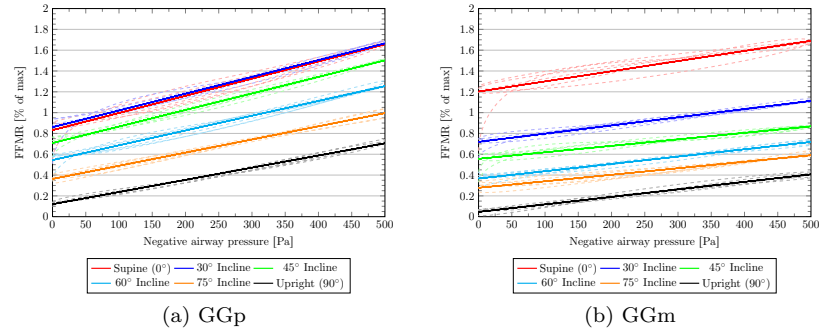


Figure 13: Genioglossus response to change in posture

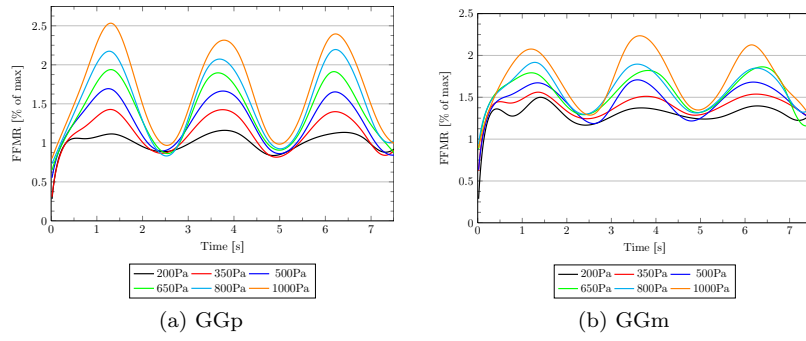


Figure 14: Genioglossus response to change in minimum epiglottal pressure

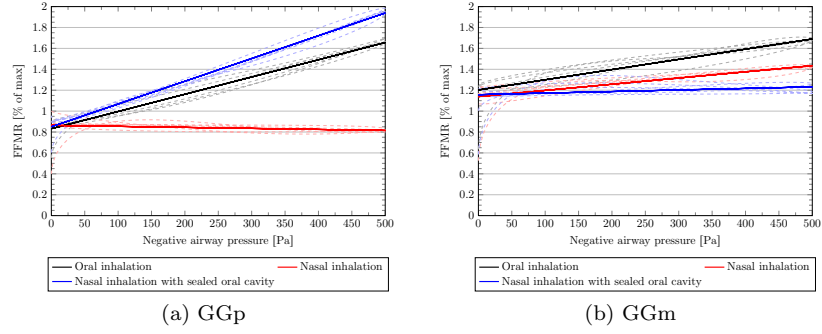


Figure 15: Genioglossus response to change in inhalation method (pressure distribution)

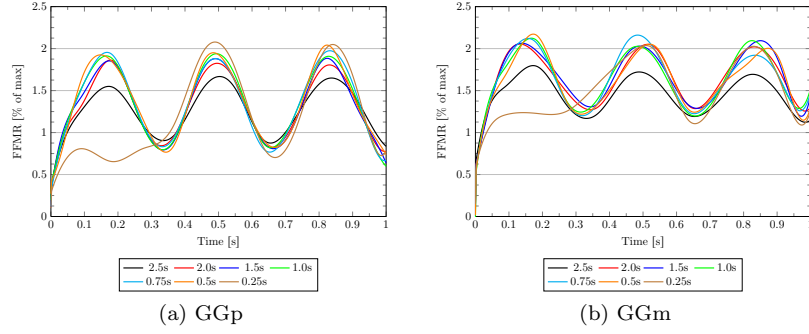


Figure 16: Genioglossus response to change in speed of inhalation. The time over which each inhalation occurs has been normalized so that results are comparable between each case. During the first cycle at the shortest period, the neural model was not able to respond rapidly enough, resulting in a poor predicted response. However, in the latter two simulated breaths the response was adequate.

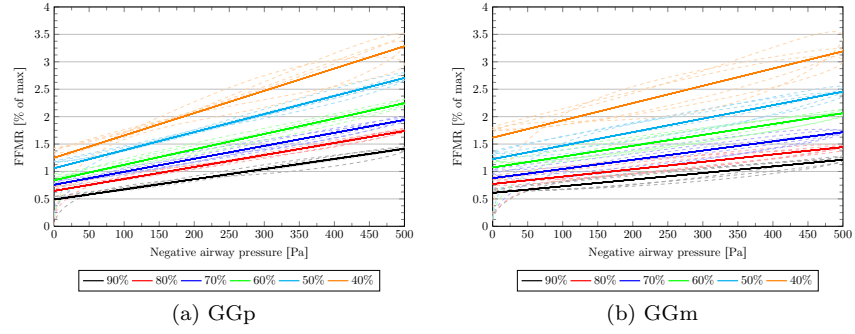


Figure 17: Genioglossus response to change in tongue adipose tissue content